

SI Appendix

Supplementing Results and Discussion

Sequence dataset specification

We obtained 1,486,735 bacterial and 796,544 archaeal sequences (Table S2) and 174,820 bacterial and 16,896 archaeal operational taxonomic units at 97% sequence identity level (OTU_{0.03}). OTU_{0.03} that occurred only once in the whole dataset are termed absolute single sequence OTU_{0.03} (SSO_{abs}) (1). OTU_{0.03} that occurred only once in at least one sample, but are more frequent in other samples are termed relative single sequence OTU (SSO_{rel}) (1). The archaeal dataset contained 55% SSO_{abs} and 19% SSO_{rel} and the bacterial dataset contained 58% SSO_{abs} and 22% SSO_{rel}. Richness estimates and the number of SSO_{rel} per sampling site (Table S1) were similar to values reported before in local studies of benthic habitats (1, 2). To test the quality of the dataset we compared our results to those of previous studies. The relative sequence abundance of all ANME clades matched well with relative sequence abundances obtained by 16S rRNA gene libraries and relative cell abundances determined by fluorescence *in situ* hybridization (FISH) (Table S11). Thus, the considerations based on the 454 data may be extended to the *in situ* abundance of ANME clades.

Methane seeps enhance seafloor biodiversity

Microbial richness and evenness of seafloor ecosystems

With a value of D close to 1, archaeal diversity was extremely low at some methane seeps and hydrothermal vents, i.e. the gas- and mud-emitting Håkon Mosby mud volcano (HMMV; D=1.2) and the Lost City hydrothermal vents (LC2, LC4; D=1.4); it was highest in intertidal microbial mats of the North Sea coast (MM3; D=64). Bacterial diversity was also lowest at seeps and vents, i.e. at a chimney of the Lau Vent Field (LV5; D=3.9), and at an extinct methane seep in Antarctica (ANT; D=4.5). It peaked in deep-sea surface sediments in the southeast Pacific off New Zealand (NZS9; D=719). Across all benthic ecosystems, archaeal diversity was lower than bacterial diversity, as previously observed for other microbiomes, e.g. of subglacial sediments (3). On average archaeal S, Chao1 and D were, respectively, 4-, 6- and 15-fold lower than that of bacteria.

The wide span of microbial diversity observed across all seep sites is best explained by differences in local heterogeneity. Low-diversity methane seep communities were predominantly found in deep sediment layers of seeps (DS; Fig. 2A), at seeps overlaid by

anoxic waters (BS) or hot seeps (GB) where the number of niches available to microbes is reduced (4, 5), and/or the pool of colonists to select from is smaller. Complex seep communities tended to be associated with productive ocean regions at depths of 400-1000 m, and with the presence of rich animal communities (e.g. QS, GoM, NZ, HR). Interestingly, although relatively few bacterial and archaeal taxa are capable of metabolizing methane directly, we showed that the overall microbial community diversity sustained at seeps is high, and different from that of the surrounding seafloor and hydrothermal vents.

Microbial community similarity between seafloor ecosystems

Community dissimilarity was lowest in deep-sea surface sediments, which shared a high proportion of bacterial taxa (Fig. 2B/C; Table S1, S4). As an example, two samples from methane seeps of the same region at Guaymas Basin (GB1 and GB2) were less similar in community structure than deep-sea sediments from different hemispheres (NZS and SMS), or sands from a Hawaiian coral reef and the North Sea (e.g. CR2 and MM3).

We tested the differences between seafloor ecosystems using random subsampling and permutation-based Redundancy Analysis (RDA; $N_{\text{test}}=10$, $p_{\text{threshold}}<0.05$) including correction for false positives (6). All seafloor ecosystems were significantly different from each other using pairwise comparisons of either archaeal or bacterial communities. In addition, we tested whether cold-temperature methane seeps, hot methane seeps and SMTZ were significantly different from each other. Indeed, for nearly all tested combinations both the archaeal and bacterial community structures differed significantly. Only the bacterial communities of SMTZ were not significantly different from those of hot and cold seeps, confirming earlier observations (7).

Microbial community composition of seafloor ecosystems

Indicator taxa for each ecosystem (Table S5) were calculated based on the relative frequency of occurrence and relative abundance (8). Lau Vent Field samples (LV1-6) stood out due to the occurrence and high sequence abundance of *Epsilonproteobacteria*, which can be explained by their role in sulfide oxidation under different environmental conditions (9). Deep-sea surface sediments (NZS, SMS) in our study were characterized by the presence of *Gemmatimonadetes* and *Acidobacteria*, consistent with previous findings (10). Heterotrophic *Bathyarchaeota* (formerly Miscellaneous Crenarchaeotic Group) (11, 12) and *Chloroflexi* (13) are typical for organic-rich subsurface ecosystems. *Methanomicrobia* and *Deltaproteobacteria* as well as candidate divisions Hyd24-12 and JS1 (Fig. 3) were typical for methane seeps.

In addition, we found other core microbial clades at methane seeps with unknown function. These clades included *Thermoplasmatales*, which were shown to comprise methane-metabolizing organisms (14), and *Firmicutes* that include sulfate reducers (15). The *Spirochaetes* may be favored at sulfide-rich methane seeps, since they contain sulfide-oxidizers that live in consortia with sulfate-reducing bacteria (16). Organisms of candidate division JS1 were present at all sites and constituted the dominant clade at some hot seeps (GB) and all deep mud volcano sediments (DS) (Fig 3; Fig. S5B). JS1 is also widespread in subsurface methane hydrates and organic-rich shelf sediments (17), indicating an overlap between the communities of these ecosystems. JS1 organisms are suspected to be syntrophic acetate oxidizers (18) involved in the methane-derived carbon cycle at seeps (19). In contrast to a previous study (20) we found that JS1 correlated negatively with delta-proteobacterial SRB (Spearman's rank correlation $R=-0.49$, $p<0.01$).

Environmental selection at methane seeps

On order level the available parameters sediment temperature, sediment depth, water depth, methane concentration, and space explained 16% ($p=0.018$) of the archaeal and 10% ($p=0.049$) of bacterial community variation. The archaeal community at methane seeps was shaped mainly by sediment temperature (RDA; $p_{\text{Order}}=0.01$, Figure S5A), whereas the bacterial community was shaped mainly by sediment depth ($p_{\text{Order}}=0.02$, Figure S5B). Compared to other global sampling efforts targeting microbial community assemblages, these numbers represent a large amount of explained variation. For comparison, 15 environmental parameters explained 11% of bacterial community variation in a subtropical river (21) and 12 environmental factors were needed to explain 44% of the variance in relative abundance of a single bacterial genus in soil (22). Unfortunately, no data were available for other relevant environmental factors previously found to structure microbial diversity at seeps, such as microbial interactions (23), faunal activity (24, 25) and stability of the seafloor system (26).

Supplementing Material and Methods

Primers used for amplification of the 16S rRNA V6 region

Archaeal forward primer (958F):

AATTGGANTCAACGCCGG

Archaeal reverse primers (1048R major/minor):

CGRCGGCCATGCACCWC

CGRCRGCCATGYACCWC

Bacterial forward primers (967F):

CTAACCGANGAACCTYACC

CNACGCGAAGAACCTTANC

CAACGCGMARAACCTTACC

ATACGCGARGAACCTTACC

Bacterial reverse primers (1046R):

CGACAGCCATGCANCACCT

CGACAACCATGCANCACCT

CGACGGCCATGCANCACCT

CGACGACCATGCANCACCT

The primers originate from the International Census of Marine Microbes (ICoMM), for further details see (27, 28) (<http://vamps.mbl.edu/resources/prim.php>).

Sequence processing routine

Processing of the 454 pyrosequencing amplicons was performed according to the following routine modified from Pat Schloss (29).

Step 1 - Extract data from binary file
sffinfo(sff=Data.sff, flow=T)

Step 2 – Separate flowgrams
trim.flows(flow=Data.flow, oligos=Data.oligos, pdiffs=2, bdiffs=1, processors=16)

Step 3 – Reducing sequencing error using a method based on PyroNoise (30)
shhh.flows(file=Data.flow.files, processors=16)

Step 4 - Concatenate single files to make one file containing all samples:
cat *.trim.shhh.fasta > AllArch.fasta
cat *.trim.shhh.names > AllArch.names
cat *.trim.shhh.groups > AllArch.groups

Step 5 - Trim sequences using minlength=75 (for bacteria), 80 (for archaea):
trim.seqs(fasta=All.fasta, name=All.names, oligos=Data.oligo, pdiffs=1, bdiffs=0, maxhomop=8, minlength=80, flip=F, processors=16)

Step 6 - Find unique sequences:
unique.seqs(fasta=All.trim.fasta, name=All.trim.names)

Step 7 - Align sequences:
align.seqs(fasta=All.trim.unique.fasta, reference=silva.archaea.fasta, processors=16) #for bacteria use (silva.bacteria.fasta)

Step 8 - Screen sequences:
screen.seqs(fasta=All.trim.unique.align, name=All.trim.names, group=All.groups, optimize=start-end, criteria=90)

Step 9 - Filter dataset:
filter.seqs(fasta=All.trim.unique.good.align, vertical=T, trump=., processors=16)

Step 10 - Simplify the dataset:
unique.seqs(fasta=All.trim.unique.good.filter.fasta, name=All.trim.good.names)

Step 11 – Preclustering based on single-linkage preclustering (31)
pre.cluster(fasta=All.trim.unique.good.filter.unique.fasta, name=All.trim.unique.good.filter.names, group=All.good.groups, diffs=0)

Step 12 - Chimera check using uchime (32):
chimera.uchime(fasta=All.trim.unique.good.filter.unique.precluster.fasta, name=All.trim.unique.good.filter.unique.precluster.names, group=All.good.groups, processors=16)

Step 13 - Chimera removal:
remove.seqs(accnos=All.trim.unique.good.filter.unique.precluster.uchime.accnos, fasta=All.trim.unique.good.filter.unique.precluster.fasta, name=All.trim.unique.good.filter.unique.precluster.names, group=All.good.groups)

Step 14 - Classify sequences:
classify.seqs(fasta=All.trim.unique.good.filter.unique.precluster.pick.fasta, template=nogap.archaea.fasta, taxonomy=silva.archaea.silva.tax) # for bacteria use (nogap.bacteria.fasta, taxonomy=silva.bacteria.silva.tax)

Step 15 - Remove lineages:
remove.lineage(fasta=All.trim.unique.good.filter.unique.precluster.pick.fasta, name=All.trim.unique.good.filter.unique.precluster.pick.names, group=All.good.pick.groups, taxonomy=All.trim.unique.good.filter.unique.precluster.pick.silva.taxonomy, taxon=Bacteria) # or remove Eukarya/Archaea

Step 16 - Simplify names:
system(cp All.trim.unique.good.filter.unique.precluster.pick.silva.pick.taxonomy All.taxonomy)
system(cp All.trim.unique.good.filter.unique.precluster.pick.pick.fasta All.fasta)
system(cp All.trim.unique.good.filter.unique.precluster.pick.pick.names All.names)
system(cp All.good.pick.pick.groups All.groups)

Step 17 - Distance matrix:
dist.seqs(fasta=All.fasta, cutoff=0.15, processors=16)

Step 18 - Cluster:
cluster(column=All.dist, name=All.names)

Step 19 - Get data for 0.03:
make.shared(list=All.an.list, group=All.groups, label=0.03)

Step 20 - Normalize the number of sequences in each sample:
count.groups() # subsample according to the smallest group size
sub.sample(shared=All.an.shared, size=3000)

Step 21 - Consensus taxonomy for each OTU:
classify.otu(list=All.an.list, name=All.names, taxonomy=All.taxonomy, label=0.03, cutoff=80)

Step 22 - OTU-based analysis Alpha diversity:
collect.single(shared=All.an.0.03.subsample.shared, calc=sobs-chao-invsimpson, freq=100)
summary.single(shared=All.an.0.03.subsample.shared, calc=nseqs-coverage-sobs-invsimpson)

Data analyses

The original subsampled sequence abundance tables were used to calculate Inverse Simpson diversity indices (33) and Chao1 richness (34) using mothur v24. Dissimilarities between all samples were calculated using the Bray-Curtis dissimilarity coefficient (i.e. relative sequence abundance) (35). The resulting beta-diversity matrices were used for 2-dimensional non metric multidimensional scaling (NMDS) ordinations with 20 random starts (36). Stress values below 0.2 indicate that the multidimensional dataset is well represented by the 2D ordination. To test whether the inclusion of singletons affected further statistical tests we generated NMDS ordinations with and without absolute singletons (SSO_{abs}) and compared them using Procrustes correlation analysis (37). The correlation of the two archaeal (Procrustes correlation coefficient=0.999, $p=0.001$) and the two bacterial ordinations (0.998, $p=0.001$) was highly significant, meaning that the presence of SSO_{abs} did not affect the overall trend. Thus we decided to include the singletons in our analyses, to be able to identify types of microorganisms which can switch from rare to dominant modes of distribution. Taxa that were shared between ecosystems and samples were calculated using the Jaccard dissimilarity coefficient (i.e. presences absence). RDA (Redundancy Analyses) based on Hellinger transformed OTU_{0.03} datasets (38) were carried out to evaluate the combined effects of sediment depth, sediment temperature, water depth and ranges of methane and sulfate concentrations on the microbial community composition in methane seep habitats. The significance of combined and pure effects was assessed by analysis of variance (ANOVA). Indicator taxa of the different seafloor microbiomes were calculated based on relative abundance tables (8). Distance decay was based on pairwise community dissimilarities using the Sørensen index and assessed in a logarithmic transformed space to enhance the linear fitting (39). Log-transformations were done using the natural logarithm, which gives the same results than log₁₀ transformations (40). Because some values were zero in the similarity and distance tables, a small value (0.01) was added before log-transformation (41). The significance of β was tested by 1000 Monte Carlo permutations of the residuals under the full regression model (38). The network was based on presence absence tables. The network vertices (nodes) were plotted using a Fruchterman and Reingold force-directed algorithm (42), which causes an increase in the nodes attraction to each other with increasing similarity between them. For our dataset, it means that the more OTU_{0.03} two samples share, the closer they are placed in the network. All analyses were carried out with the R statistical environment and the packages *vegan* (43), *labdsv* (44), *gmt* (45), *network* (46), and with custom R scripts.

Supplementing Figures

Figure S1

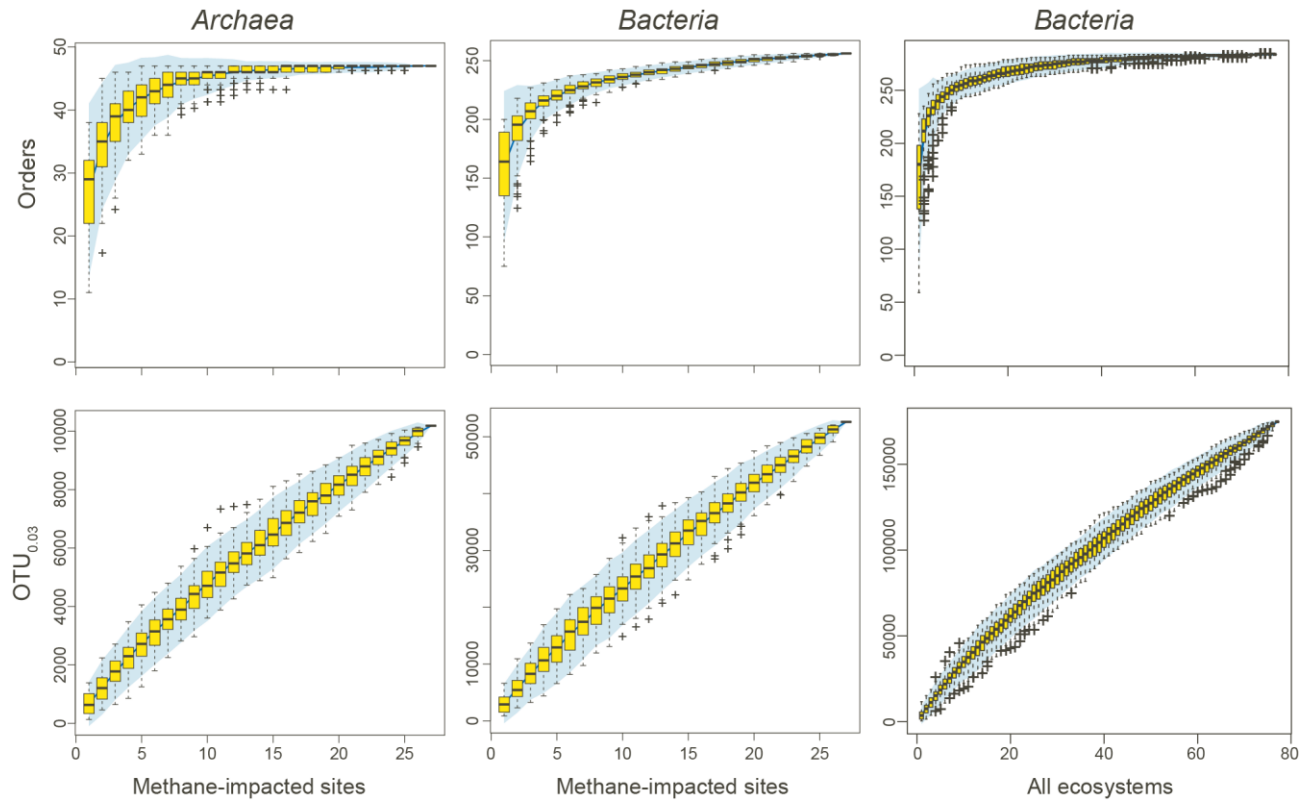


Figure S1: Species accumulation curves of *Archaea* and *Bacteria*

Species accumulation curves based on archaeal (left) and bacterial (middle) orders (upper panel) and OTU_{0.03} (lower panel) detected at the 27 methane-impacted ecosystems (23 methane seeps and 4 SMTZ); as well as for bacterial orders and OTU_{0.03} (right) for all 77 investigated ecosystems. The boxplots show a summary of 100 permutations that were calculated for each point using Chao1 richness and random subsampling. The blue area depicts the 95% confidence interval. Extrapolation of species richness using the Chao1 estimator based on the whole dataset indicated that around $361,000 \pm 1,500$ (\pm SEM) bacterial and $33,000 \pm 470$ archaeal OTU_{0.03} inhabit the investigated seafloor habitats.

Figure S2

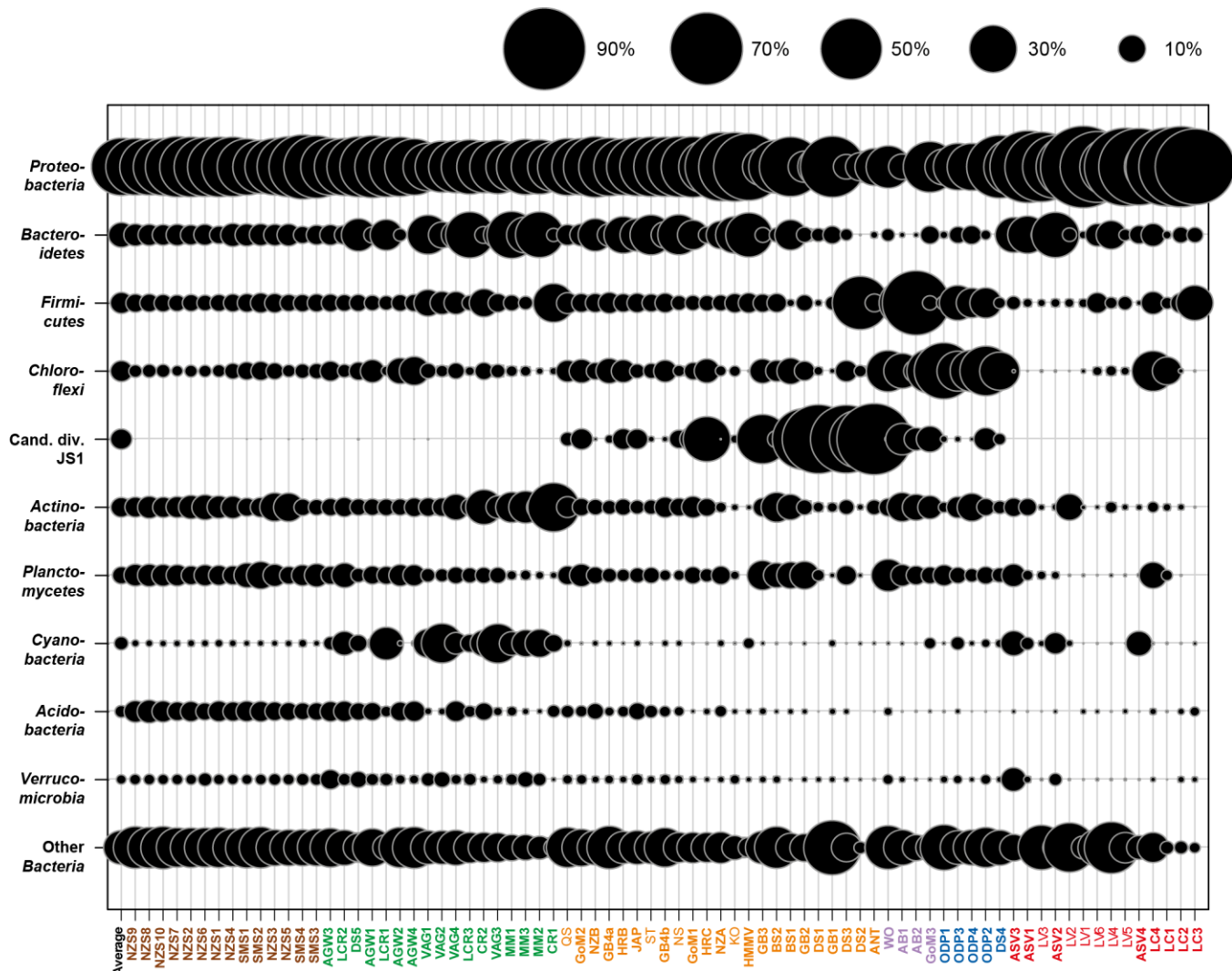


Figure S2: Relative abundance of bacterial phyla

Seven of the ten phyla were cosmopolitan. Candidate division JS1 basically occurred only at methane seeps, SMTZ and in the subsurface. *Acidobacteria* were detected in all, but two samples (DS2, LV2) and *Planctomycetes* were detected in all, but one sample (LC3).

Figure S3

A

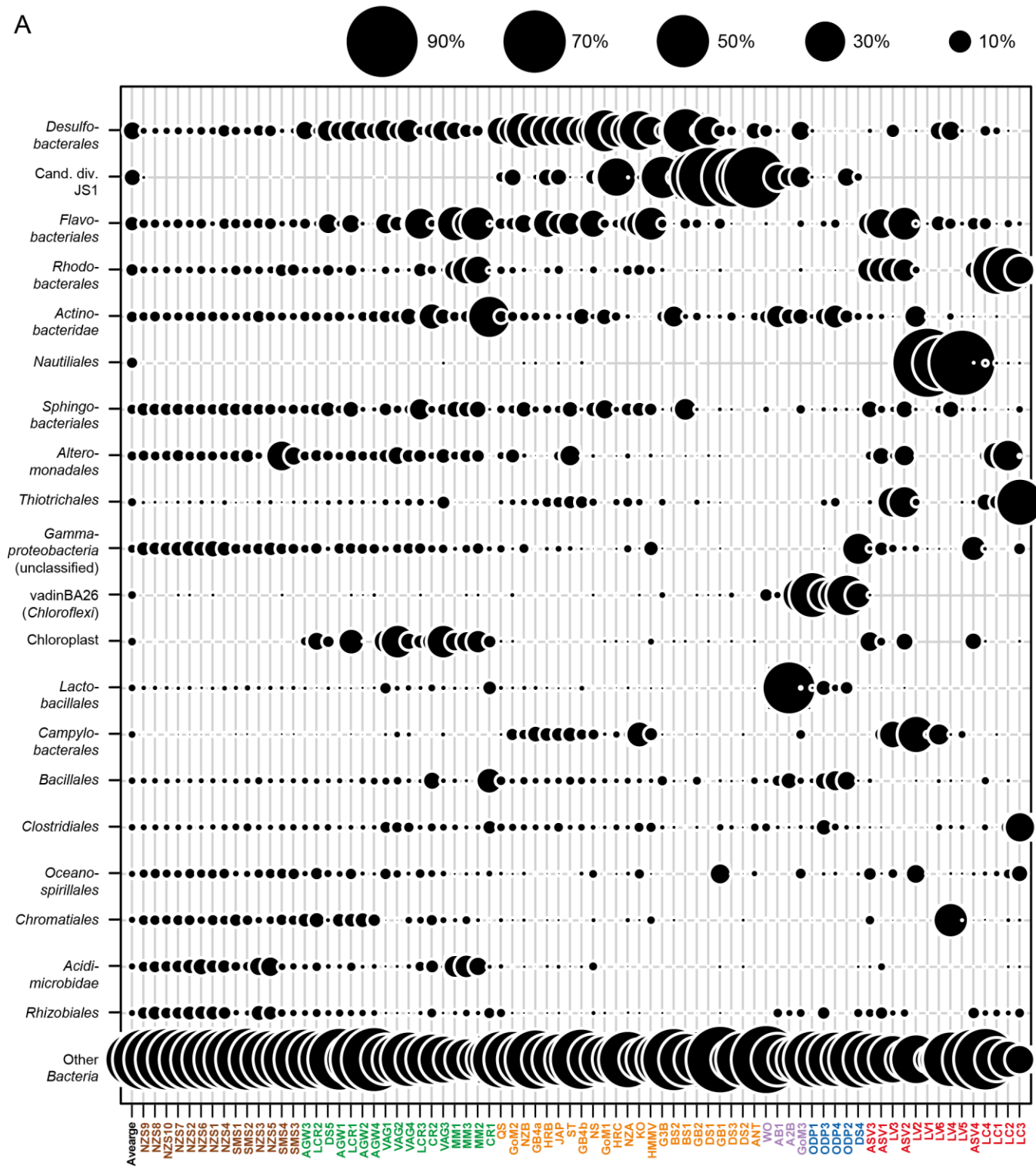


Figure S3

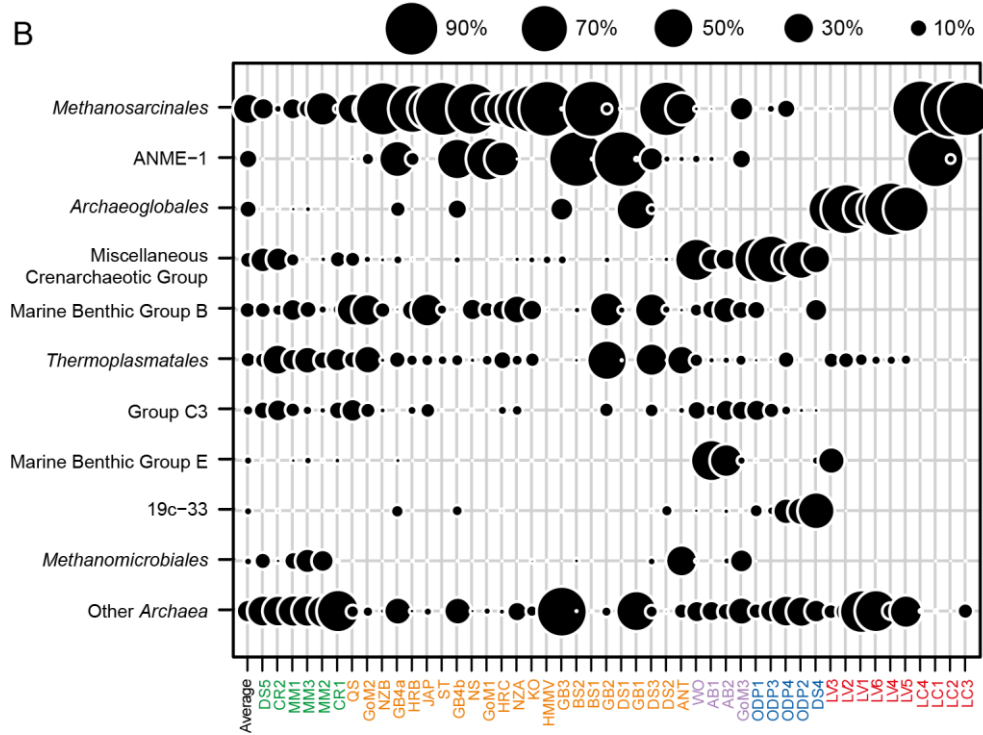


Figure S3: Relative abundance of bacterial and archaeal orders

Relative sequence abundances of bacterial (A) and archaeal orders (B) at all investigated sites.

Figure S4

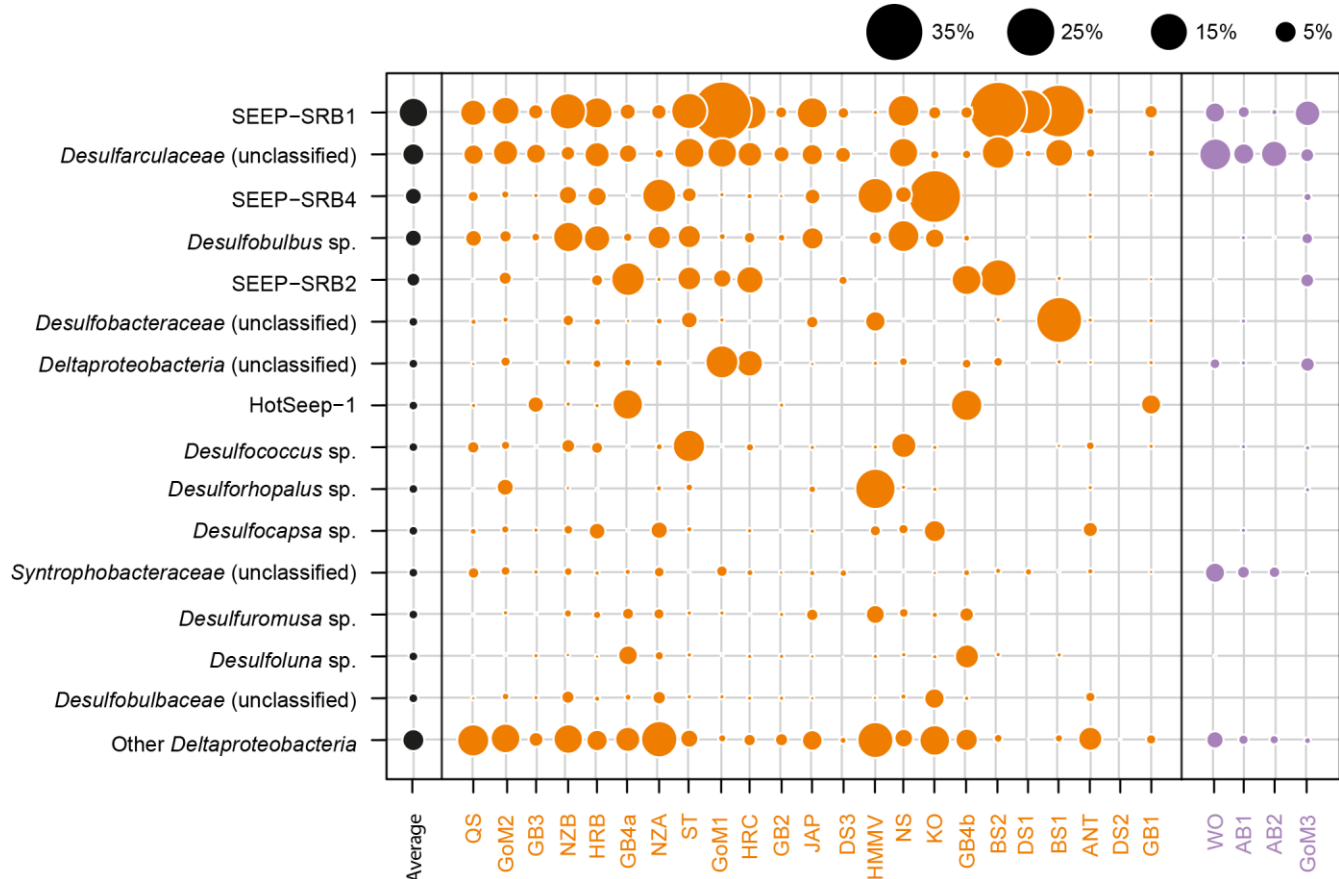
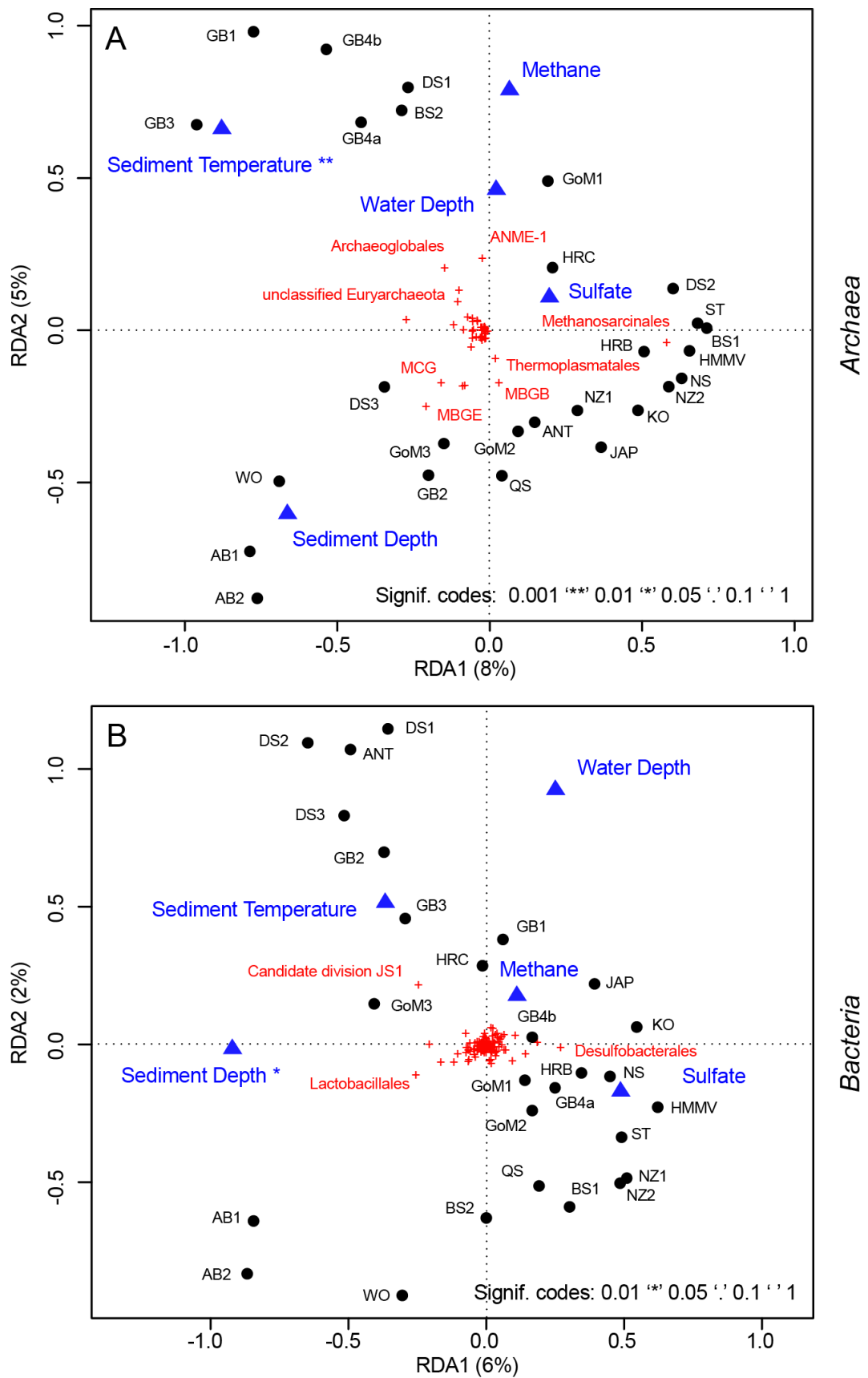


Figure S4: Relative abundance of Deltaproteobacteria and HotSeep-1

Most methane-rich sites were dominated by SEEP-SRB1 (*Desulfobacteraceae*), which are known to form consortia with the ANME-2 clade (47). Other ANME partner SRB include SEEP-SRB2 (48) and HotSeep-1 from Guaymas Basin hydrothermal sediments (49). *Desulfarculaceae* and SEEP-SRB4 (*Desulfobulbaceae*) both frequently occur at seep ecosystems, but were not shown to aggregate with ANME. The taxonomic classification of deltaproteobacterial subgroups is based on SILVA (release 119, 07-2014; (50)).

Figure S5



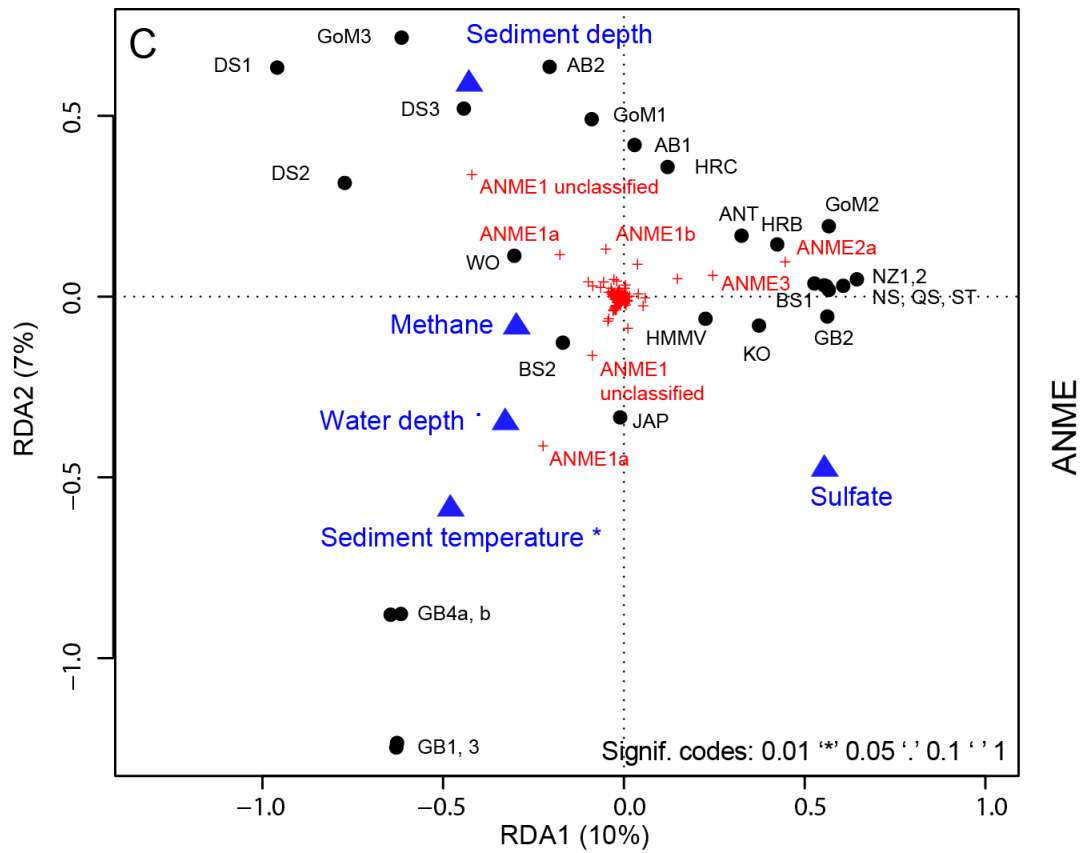


Figure S5: Redundancy analysis of archaeal and bacterial diversity

Redundancy analysis (RDA) using the relative abundance of archaeal orders (**A**), bacterial orders (**B**) and ANME OTU_{0.03} (**C**), and five environmental parameters of 27 methane-impacted ecosystems (23 methane seeps and 4 SMTZ). The plots show the full model considering all five parameters, which was highly significant in all cases. Black circles represent the microbial community of a given sample, environmental parameters are fitted to the ordination and represented as blue triangles. Microbial orders or OTU_{0.03} are depicted as red crosses. Note: In RDA plots environmental parameters and species are generally shown as centered arrows originating in point 0/0 (which represents the average and not zero). To simplify the plot we show the tips of the arrows as blue triangles or red crosses. Significance levels (marked by asterisks) were calculated for each parameter on its own using partial RDA.

Figure S6

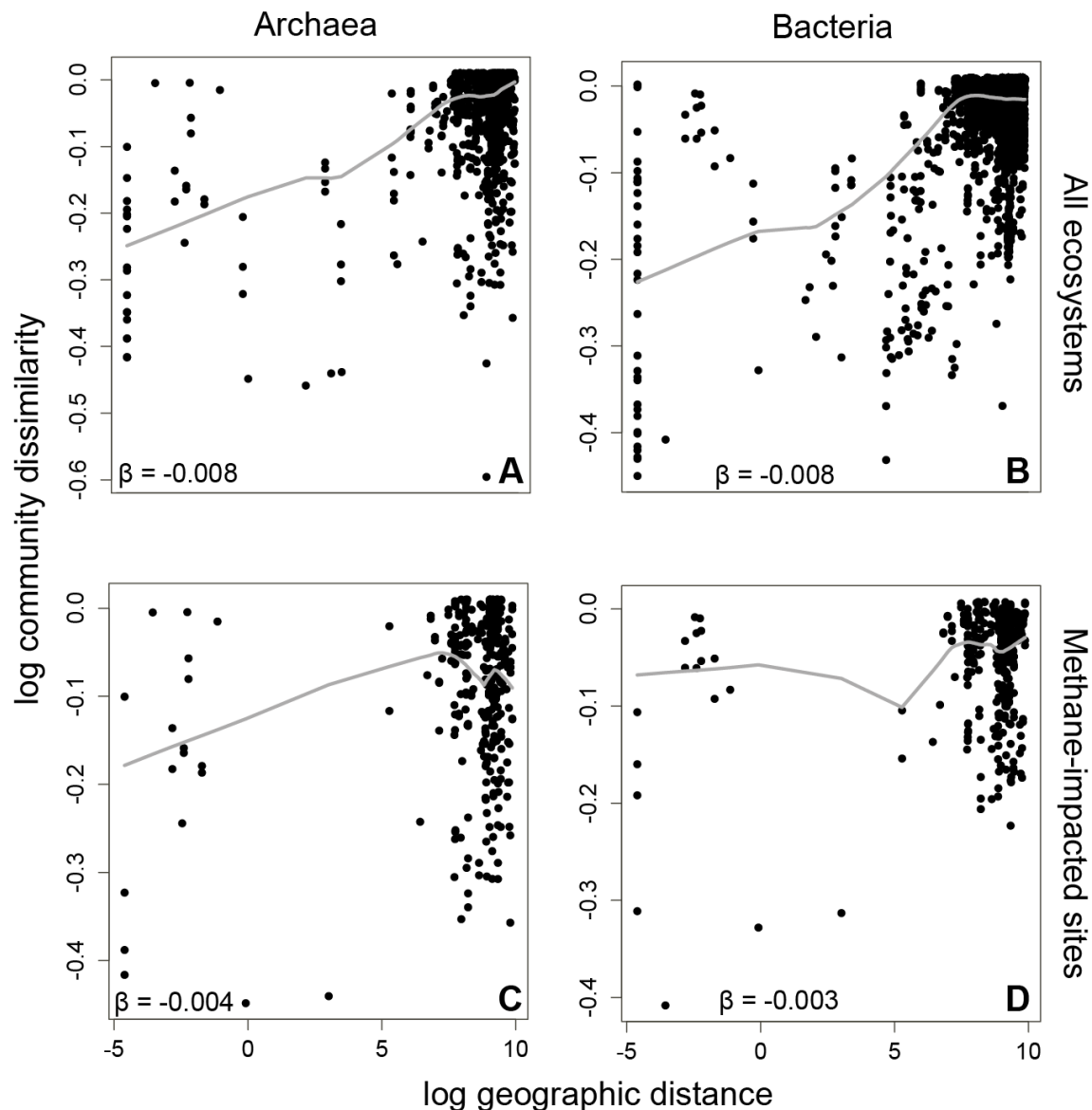


Figure S6: Distance decay of microbial community similarity

Distance decay (DD) of community similarity was calculated based on geographic and community distance matrices. The plots show decreasing microbial community similarity (from top to bottom; y-axis) with increasing geographic distance (from left to right; x-axis). (A) and (C) show archaeal communities, (B) and (D) bacterial communities. The global dataset is shown in (A) and (B), whereas AOM habitats (23 methane seeps and four SMTZ) are represented by (C) and (D). The regression was calculated using a linear model. The slope β of each regression was highly significant ($p < 0.001$) as determined by ANOVA and 1000 permutations.

Figure S7

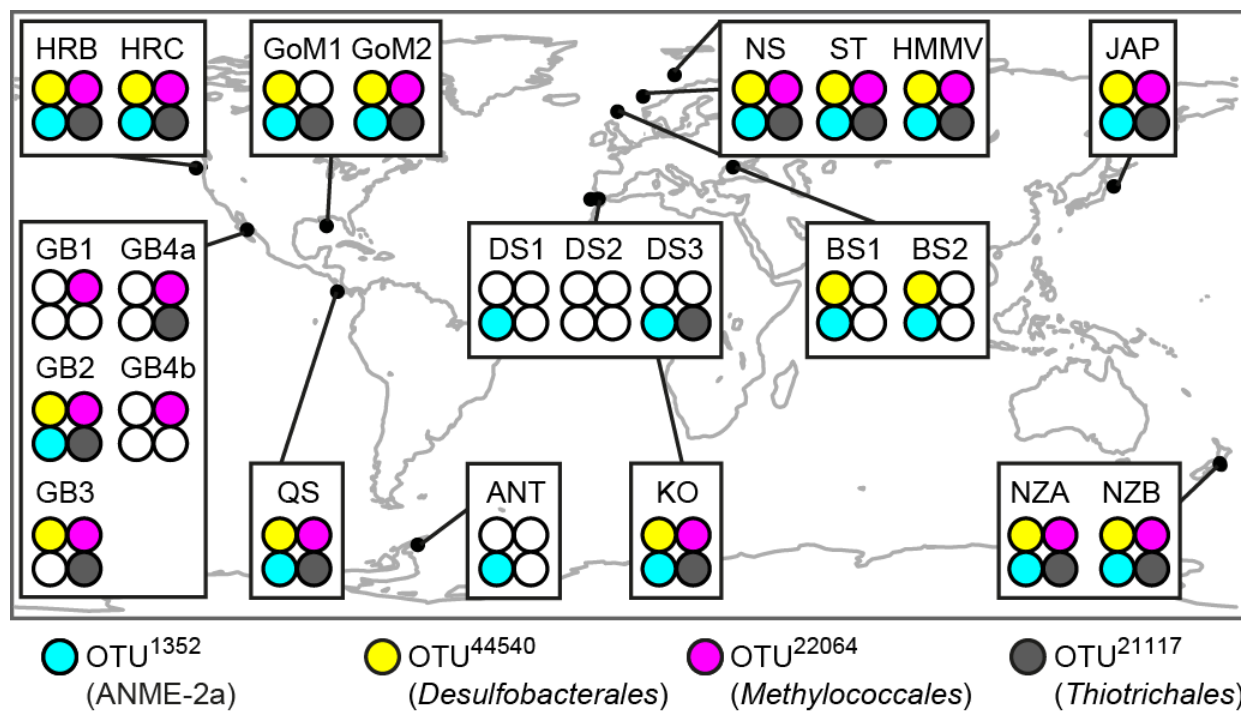


Figure S7: Global occurrence of OTU_{0.03} from key functional taxa

The most widespread and also most sequence-abundant ANME OTU_{0.03} belonged to clade ANME-2a and occurred at 18 of 23 cold seeps. The most widespread OTU_{0.03} of sulfate-reducing *Desulfobacterales*, aerobic methanotrophic *Methylococcales* and sulfur-oxidizing *Thiotrichales* each occurred at 16 of 23 cold seeps. These four OTU_{0.03} were present at basically all sites where methane, sulfate and oxygen were available and the temperature was around 4°C. At anoxic, sulfate-rich sites (BS1, 2) only the two anaerobic OTU_{0.03} belonging to ANME and sulfate-reducing bacteria (SRB) were present. Sediments from Guaymas Basin that include warm (15-25°C; GB1-2) or even hot sites (> 50°C; GB3, GB4b) lacked these two OTU_{0.03}. Here, AOM is carried out by thermophilic ANME and SRB (4). For the frequency of the top 10 OTU_{0.03} from each of the four clades see Table S9.

Table S1: Characteristics of seafloor microbiomes

	Average Observed Richness (S)	Average Estimated Richness (Chao1)	Average Inverse Simpson Index (D)	Average SSOabs per sample (in %)	Average SSOrel per sample (in %)	Beta-dispersion **	Most frequent class ***	Most frequent order ***	Indicator class ****	Domain contribution to S/Chao1 (in %)	
Bacteria	Deep-Sea Surface (14)*	1720	6447	445	30	34	0.47	Gamma-proteobacteria	<u>Alteromonadales</u>	SAR202 (<i>Chloroflexi</i>)	n.a.
	Coastal Sediments (17)	1458	4634	247	35	26	0.62	Gamma-proteobacteria	Flavobacteriales #	OPB35 #	46/51
	Methane Seeps (23)	847	2499	87	34	24	0.64	Delta-proteobacteria	Candidate division JS1	Delta-proteobacteria	74/77
	SMTZ (4)	782	2166	87	38	18	0.68	Bacilli	Lactobacillales	GIF9 (<i>Chloroflexi</i>)	56/66
	Subsurface (5)	750	1585	78	35	16	0.52	vadinBA (<i>Chloroflexi</i>)	vadinBA26 (<i>Chloroflexi</i>)	vadinBA (<i>Chloroflexi</i>)	83/83
	Hydrothermal Vents (14)	465	1152	28	33	21	0.65	Gamma-proteobacteria	Nautiliiales	Epsilon-proteobacteria	70/64
Archaea	Deep-Sea Surface (0)*	n.a.	n.a.	n.a.	n.a.	n.a.	n.a.	n.a.	n.a.	n.a.	n.a.
	Coastal Sediments (6)	617	1558	46	43	14	0.55	Methanomicrobia##	Thermoplasmatales	Marine Group 1	54/49
	Methane Seeps (23)	210	492	7.5	28	24	0.62	Methanomicrobia	Methanomicrobia	Methanomicrobia	26/23
	SMTZ (4)	305	635	13	31	19	0.68	Thermoplasmata	MBGE	SCG	44/34
	Subsurface (5)	130	269	7.0	33	18	0.44	MCG	MCG	Methanopyri	17/17
	Hydrothermal Vents (10)	119	307	4.2	34	20	0.56	Methanomicrobia	Archaeoglobales	Thermococci	30/36

SSOrel/abs: Relative/absolute single sequence OTU_{0.03}

S, Chao1 and D were standardized based on resampling of 3000 sequences

n.a. not analyzed * Number of samples

** Average within group dissimilarity based on distance to centroid, p<0.01 (permtest)

*** Based on relative 16S rRNA (V6) sequence abundance using pyrosequencing

**** Based on rel. abundance/rel. frequency of occurrence (8)

Taxonomic assignment based on SILVA release 102 (50)

SMTZ: Sulfate methane transition zone

Chloroplast sequences targeted by the primers were originally the most frequent order and indicator class, but were discarded as they originate from algae and plants

Methanomicrobia of coastal sands almost exclusively contained methanogens, Methanomicrobia of cold seeps were comprised of ANME

MCG: Miscellaneous Crenarchaeotic Group

Table S2: Diversity parameters of seafloor samples

	Quality Reads		OTU _{0,03}		OTU _{0,03} **		Inverse Simpson **		Chao1 Richness **	
Sample *	Bacteria	Archaea	Bacteria	Archaea	Bacteria	Archaea	Bacteria	Archaea	Bacteria	Archaea
NZS9	33365	n.a.	11671	n.a.	1978	n.a.	719	n.a.	8848	n.a.
NZS8	19900	n.a.	8710	n.a.	1980	n.a.	604	n.a.	8409	n.a.
NZS10	28897	n.a.	10157	n.a.	1902	n.a.	600	n.a.	8286	n.a.
NZS7	20901	n.a.	7310	n.a.	1821	n.a.	537	n.a.	7681	n.a.
NZS2	25783	n.a.	8483	n.a.	1759	n.a.	412	n.a.	6865	n.a.
NZS6	25882	n.a.	7854	n.a.	1667	n.a.	364	n.a.	6317	n.a.
NZS1	17715	n.a.	6348	n.a.	1687	n.a.	371	n.a.	6297	n.a.
NZS4	26337	n.a.	8652	n.a.	1713	n.a.	375	n.a.	6078	n.a.
SMS1	27080	n.a.	7926	n.a.	1747	n.a.	521	n.a.	5831	n.a.
SMS2	18150	n.a.	6223	n.a.	1704	n.a.	515	n.a.	5571	n.a.
NZS3	20111	n.a.	6223	n.a.	1588	n.a.	399	n.a.	5482	n.a.
NZS5	33401	n.a.	8572	n.a.	1530	n.a.	357	n.a.	5268	n.a.
SMS4	21233	n.a.	5551	n.a.	1471	n.a.	179	n.a.	4702	n.a.
SMS3	27652	n.a.	6881	n.a.	1532	n.a.	273	n.a.	4620	n.a.
AGW3	23538	n.a.	7333	n.a.	1726	n.a.	338	n.a.	6377	n.a.
LCR2	4701	n.a.	2607	n.a.	1869	n.a.	526	n.a.	6264	n.a.
DS5	34012	16262	8973	1641	1665	592	524	45	6138	1687
AGW1	35557	n.a.	9184	n.a.	1662	n.a.	297	n.a.	5729	n.a.
LCR1	15171	n.a.	4704	n.a.	1629	n.a.	306	n.a.	5275	n.a.
AGW2	20162	n.a.	5721	n.a.	1573	n.a.	180	n.a.	5263	n.a.
AGW4	18389	n.a.	5362	n.a.	1597	n.a.	214	n.a.	5261	n.a.
VAG1	18488	n.a.	5385	n.a.	1527	n.a.	274	n.a.	4742	n.a.
VAG2	17942	n.a.	4730	n.a.	1335	n.a.	76	n.a.	4710	n.a.
VAG4	19473	n.a.	5450	n.a.	1553	n.a.	330	n.a.	4637	n.a.
LCR3	25604	n.a.	6465	n.a.	1513	n.a.	285	n.a.	4474	n.a.
CR2	12408	11287	3849	988	1546	549	188	52	4301	996
VAG3	14784	n.a.	4220	n.a.	1408	n.a.	96	n.a.	4147	n.a.
MM1	22933	5065	4945	1003	1213	693	186	58	3844	1755
MM3	19353	5327	4364	1203	1252	812	204	64	3302	2617
MM2	15528	3098	3224	509	1053	502	151	37	2992	1265
CR1	10763	7711	1273	898	661	553	19	19	1330	1028
QS	16005	21950	5351	1386	1613	420	462	12	5145	1106
GoM2	14048	14622	4444	650	1575	284	371	19	5035	687
GB3	12074	22525	3167	1095	1131	329	32	11	4554	809
NZB	27493	22973	6626	585	1330	181	182	3,5	4207	395
HRB	30463	33665	5810	1199	1131	257	120	7,9	3850	690
GB4a	21617	9254	4510	726	1206	401	128	19	3838	904
NZA	18425	24541	3947	1015	1135	265	51	7,8	3446	615
ST	22912	15043	3498	216	990	93	97	1,7	2844	159
GoM1	17754	14365	2897	336	874	164	58	9,4	2762	394
HRC	26048	30925	4340	1149	947	296	54	18	2726	737
GB2	20146	25446	3011	1087	830	311	11	12	2558	831
JAP	25785	21080	3856	631	921	196	121	6,1	2549	577
DS3	9578	23015	1540	832	711	252	7,6	11	2065	538
HMMV	53605	15385	3668	217	664	78	35	1,2	1777	136
NS	16765	25963	2099	485	690	153	67	2,1	1691	325
KO	12446	10074	1498	333	650	177	38	3,3	1600	371
GB4b	9018	12600	1515	691	817	315	87	10	1529	578
BS2	17392	13739	1726	134	569	57	30	1,6	1497	128
DS1	17217	18271	1040	268	331	97	11	1,8	973	183
BS1	20351	25498	1234	302	376	108	17	1,5	842	178
ANT	27721	20516	1166	397	355	133	4,5	5,6	781	333
DS2	22472	9738	865	130	279	80	6,8	1,9	616	186
GB1	19779	11865	955	440	360	174	8,8	4,4	583	463
WO	14375	16394	4190	953	1499	421	296	20	4217	846
AB1	19101	17460	1893	699	562	245	17	3,8	1760	452
AB2	18755	22592	1553	830	480	284	5,2	7,6	1407	739
GoM3	12364	6182	1206	385	588	269	28	18	1281	501

ODP1	13391	24002	1937	550	842	176	99	9,3	1860	348
ODP3	16565	16182	2201	301	909	119	120	6,0	1827	250
ODP4	12336	7267	1629	186	726	124	68	11	1536	257
ODP2	17006	15651	1791	177	676	69	70	3,7	1462	151
DS4	12996	12822	1326	383	598	161	34	4,8	1240	339
ASV3	18023	n.a.	2773	n.a.	896	n.a.	146	n.a.	2388	n.a.
ASV1	8456	n.a.	1424	n.a.	721	n.a.	80	n.a.	2088	n.a.
LV3	16556	5135	1779	236	634	178	17	4,9	1886	368
ASV2	17300	n.a.	1958	n.a.	620	n.a.	23	n.a.	1836	n.a.
LV2	12080	9232	1014	203	439	122	14	1,9	1096	221
LV1	21468	12267	1595	402	440	186	5,2	12	1065	547
LV6	25264	12488	1529	512	460	203	18	12	1027	635
LV4	7212	15068	763	241	477	95	19	1,5	1016	223
LV5	18148	12756	1017	387	376	154	3,9	3,1	918	353
ASV4	17881	n.a.	950	n.a.	331	n.a.	7,5	n.a.	793	n.a.
LC4	6973	24435	625	193	414	59	25	1,4	750	329
LC1	8165	27510	492	192	291	64	15	2,4	534	91
LC2	3688	30829	263	195	239	54	10	1,4	395	171
LC3	14305	16469	380	239	173	73	9,0	1,8	337	126

OTU_{0,03}: Operational taxonomic unit at 97% 16S rRNA V6 gene sequence identity

n.a. not available

*sorted according to decreasing Chao 1 Richness

**standardized numbers based on subsampling of 3000 sequences without replacement

Table S3: Percentage of shared archaeal and bacterial taxa between ecosystems

	Methane Seep	SMTZ	Coastal Sediment	Deep Sea Surface	Subsurface
Shared bacterial phyla (%)	SMTZ	88			
	Coastal Sediment	98	87		
	Deep Sea Surface	94	86	96	
	Subsurface	81	83	82	82
	Hydrothermal Vent	83	85	81	80
Shared archaeal OTU _{0.03} (%) *	SMTZ	6			
	Coastal Sediment	6	7		
	Deep Sea Surface	n.a.	n.a.	n.a.	
	Subsurface	3	7	4	n.a.
	Hydrothermal Vent	2	1	1	n.a.
Shared bacterial OTU _{0.03} (%) *	SMTZ	3			
	Coastal Sediment	6	2		
	Deep Sea Surface	5	1	6	
	Subsurface	2	4	1	0
	Hydrothermal Vent	2	1	3	2

Pairwise comparison of community similarity between seafloor ecosystems based on presence absence OTU_{0.03} data.

* All comparisons were significantly different from each other based on Redundancy Analysis ($p<0.05$) using 100 permutations for each pairwise comparison and further correction for multiple testing (6).

Table S4: Percentage of shared archaeal and bacterial OTU_{0.03} between samples

	Number of samples	Domain	Max shared OTU _{0.03} (%) *	Mean shared OTU _{0.03} (%) *	Min shared OTU _{0.03} (%) *
Deep Sea Surface	14	<i>Bacteria</i>	34	19	8
	0	<i>Archaea</i>	n.a.	n.a.	n.a.
Coastal Sediments	17	<i>Bacteria</i>	38	6	<1
	6	<i>Archaea</i>	25	9	<1
Methane Seeps	23	<i>Bacteria</i>	37	5	<0.1
	23	<i>Archaea</i>	66	8	0
SMTZ	4	<i>Bacteria</i>	33	7	<1
	4	<i>Archaea</i>	49	13	4
Subsurface	5	<i>Bacteria</i>	18	10	6
	5	<i>Archaea</i>	28	18	13
Hydrothermal Vent	14	<i>Bacteria</i>	29	3	0
	10	<i>Archaea</i>	78	14	0

* Pairwise comparison of community similarity within seafloor ecosystems based on presence absence OTU_{0.03} data. Values refer to maximum, mean or minimum shared OTU_{0.03} between any given pair of samples from the respective ecosystem.

n.a. not available

Table S5: Archaeal and bacterial indicator taxa for seafloor ecosystems

Microbial taxa * (class or phylum level)	Seafloor ecosystem	Indicator value **	p Value
Bacteria	SAR202 (<i>Chloroflexi</i>)	Deep Sea Surface	0.80
	<i>Verrucomicrobia</i> unclassified	Deep Sea Surface	0.74
	JTB23 (<i>Proteobacteria</i>)	Deep Sea Surface	0.71
	<i>Gemmatimonadetes</i>	Deep Sea Surface	0.67
	KD4-96 (<i>Chloroflexi</i>)	Deep Sea Surface	0.66
	OM190 (<i>Planctomycetes</i>)	Deep Sea Surface	0.64
	RB25 (<i>Acidobacteria</i>)	Deep Sea Surface	0.63
	<i>Thermomicrobia</i>	Deep Sea Surface	0.57
	<i>Acidobacteria</i>	Deep Sea Surface	0.55
	Arctic97B-4 (<i>Verrucomicrobia</i>)	Deep Sea Surface	0.47
	<i>Acidimethylsilex</i>	Deep Sea Surface	0.46
	<i>Planctomycetacia</i>	Deep Sea Surface	0.43
	Candidate division GOUTA4	Deep Sea Surface	0.42
	ML602M-17 (<i>Bacteroidetes</i>)	Deep Sea Surface	0.42
	<i>Holophagae</i>	Deep Sea Surface	0.42
	vadinHA49 (<i>Planctomycetes</i>)	Deep Sea Surface	0.42
	Chloroplast	Coastal	0.79
	OPB35 (<i>Verrucomicrobia</i>)	Coastal	0.56
	SM1A07 (<i>Bacteroidetes</i>)	Coastal	0.53
	Candidate division WS6	Coastal	0.52
	Candidate division Hyd24-12	Methane Seep	0.69
	Candidate division JS1	Methane Seep	0.64
	<i>Deltaproteobacteria</i>	Methane Seep	0.35
	GIF9 (<i>Chloroflexi</i>)	SMTZ	0.86
	<i>Chlorobia</i>	SMTZ	0.61
	vadinBA26 (<i>Chloroflexi</i>)	Subsurface	0.75
	MLE1-12 (<i>Cyanobacteria</i>)	Subsurface	0.58
	Epsilonproteobacteria	Hydrothermal Vent	0.84
Archaea	Marine Group I	Coastal	0.89
	<i>Methanobacteria</i>	Coastal	0.85
	AK31 (<i>Thaumarchaeota</i>)	Coastal	0.83
	Ancient Archaeal Group	Coastal	0.81
	pSL12 (<i>Crenarchaeota</i>)	Coastal	0.78
	South African Gold Mine Gp 1	Coastal	0.64
	pMC2A209 (<i>Crenarchaeota</i>)	Coastal	0.62
	Marine Benthic Group A	Coastal	0.45
	<i>Methanomicrobia</i>	Methane Seep	0.41
	Soil Crenarchaeotic Group	SMTZ	0.62
	<i>Methanopyri</i>	SMTZ	0.63
	Misc. Crenarchaeotic Group	Subsurface	0.58
	<i>Thermococci</i>	Hydrothermal Vent	0.59
	<i>Candidatus Korarchaeum</i>	Hydrothermal Vent	0.57
	<i>Archaeoglobi</i>	Hydrothermal Vent	0.54
	<i>Methanococci</i>	Hydrothermal Vent	0.50

*Taxonomy is based on SILVA release 102 (50)

**Indicator Taxa are based on relative abundance and relative frequency of occurrence (8)

Table S6: Core bacterial orders of three seafloor ecosystems in percent relative abundance

Bacterial taxa * (order level or higher)	Deep Sea Surface	Sub- surface	Methane Seeps
<i>Acidimicrobidae</i>	3.8 **	-	-
<i>Acidobacteriales</i>	1.8	-	-
<i>Actinobacteridae</i>	2.4	4.5	2.2
<i>Alteromonadales</i>	4.0	-	-
<i>Bacillales</i>	1.2	4.5	1.3
<i>BD2-11 (Gemmatimonadetes)</i>	2.0	-	-
<i>Burkholderiales</i>	-	3.6 **	-
<i>Caldilineales</i>	-	-	1.2 **
<i>Candidate division JS1</i>	-	2.0	16.9
<i>Caulobacterales</i>	1.0	-	-
<i>Chromatiales</i>	2.5	-	-
<i>Clostridiales</i>	1.4	1.9	1.3
<i>Desulfarculales</i>	-	2.3	-
<i>Desulfobacterales</i>	1.9	-	15.1
<i>Desulfovibrionales</i>	-	1.5	-
<i>Desulfuromonadales</i>	1.9	-	-
<i>Enterobacteriales</i>	1.3	-	-
<i>Flavobacteriales</i>	2.3	-	5.1
<i>Gammaproteobacteria unclassified</i>	3.9	3.8	-
<i>GIF3 (Chloroflexi)</i>	-	2.2	-
<i>Holophagales</i>	1.2	-	-
<i>Lactobacillales</i>	-	2.2	3.0
<i>mle1-8 (Phycisphaerae)</i>	-	1.5	-
<i>Myxococcales</i>	2.3	-	-
<i>Nitrospirales</i>	1.4	-	-
<i>Oceanospirillales</i>	2.3	-	-
<i>Phycisphaerales</i>	1.0	-	-
<i>Planctomycetales</i>	1.1	-	-
<i>Proteobacteria_unclassified</i>	1.1	2.2	-
<i>Pseudomonadales</i>	-	1.8	-
<i>RB25 (Acidobacteria)</i>	1.8	-	-
<i>Rhizobiales</i>	3.2	1.2	-
<i>Rhodobacterales</i>	2.0	-	-
<i>Rhodospirillales</i>	2.4	2.1	-
<i>Sh765B-TzT-29 (Deltaproteobacteria)</i>	2.7	-	-
<i>Sphingobacteriales</i>	3.2	-	2.5
<i>Spirochaetales</i>	-	-	1.1
<i>vadinBA26 (Chloroflexi)</i>	-	22.7	-
<i>Xanthomonadales</i>	2.8	-	-

*Taxonomy is based on SILVA release 102 (50)

** Colored numbers in bold face depict relative abundances of clades that occur exclusively or with very high relative abundances in the respective ecosystem

Table S7: Contextual data of seafloor samples

Environment	Latitude	Longitude	Water depth (m)	Sediment depth (cmbsf)	T °C	CH ₄ (cat) *	SO ₄ (cat) **	Longhurst Province	Longhurst Biome	Prod. index	Climate zone	VAMPS project	Sample Code Archaea	Sample Code Bacteria	
NZS1	New Zealand Deep Sea	-43.2880	-175.5532	644	1.5	16	0	6	NEWZ	C	3	TEM	ICM_NZS	n.a.	NZS_0002
NZS2	New Zealand Deep Sea	-42.7820	-176.7142	1025	1.5	16	0	6	NEWZ	C	3	TEM	ICM_NZS	n.a.	NZS_0003
NZS3	New Zealand Deep Sea	-42.9915	175.9303	1197	1.5	15	0	6	NEWZ	C	3	TEM	ICM_NZS	n.a.	NZS_0004
NZS4	New Zealand Deep Sea	-42.9915	178.9918	530	1.5	16	0	6	NEWZ	C	3	TEM	ICM_NZS	n.a.	NZS_0005
NZS5	New Zealand Deep Sea	-44.1262	178.6445	516	1.5	14	0	6	NEWZ	C	3	TEM	ICM_NZS	n.a.	NZS_0006
NZS6	New Zealand Deep Sea	-44.4853	177.1410	1241	1.5	13	0	6	NEWZ	C	3	TEM	ICM_NZS	n.a.	NZS_0007
NZS7	New Zealand Deep Sea	-43.5195	-178.6175	424	1.5	15	0	6	NEWZ	C	3	TEM	ICM_NZS	n.a.	NZS_0009
NZS8	New Zealand Deep Sea	-44.0147	178.5190	766	1.5	14	0	6	NEWZ	C	3	TEM	ICM_NZS	n.a.	NZS_0010
NZS9	New Zealand Deep Sea	-42.5307	-178.3390	1400	1.5	16	0	6	NEWZ	C	3	TEM	ICM_NZS	n.a.	NZS_0011
NZS10	New Zealand Deep Sea	-38.6200	167.5260	482	1.5	17	0	6	TASM	W	2	TEM	ICM_NZS	n.a.	NZS_0012
SMS1	East Pacific Station M	35.1642	-123.0156	3954	5.0	1	0	6	CCAL	C	3	TEM	ICM_SMS	n.a.	SMS_0007
SMS2	East Pacific Station M	35.1642	-123.0156	3954	5.0	1	0	6	CCAL	C	3	TEM	ICM_SMS	n.a.	SMS_0008
SMS3	East Pacific Station M	35.1642	-123.0156	3954	5.0	1	0	6	CCAL	C	3	TEM	ICM_SMS	n.a.	SMS_0010
SMS4	East Pacific Station M	35.1642	-123.0156	3954	5.0	1	0	6	CCAL	C	3	TEM	ICM_SMS	n.a.	SMS_0011
DS1	Gulf of Cadiz mud volcano	35.5617	-9.5072	3860	87.5	17	4	1	CNRY	C	5	ST	ICM_CFU	CFU_02	CFU_01
DS2	Gulf of Cadiz mud volcano	35.6607	-7.3342	1326	42.5	17	4	1	CNRY	C	5	ST	ICM_CFU	CFU_04	CFU_03
DS3	Gulf of Cadiz mud volcano	35.6616	-7.3347	1326	67.5	17	4	1	CNRY	C	5	ST	ICM_CFU	CFU_06	CFU_05
GoM1	Gulf of Mexico (in mat)	28.5147	-88.2952	890	12.0	5	4	1	CARB	T	2	ST	ICM_GMS	GMS-0004	GMS-0003
GoM2	Gulf of Mexico (outside mat)	28.5147	-88.2952	890	12.0	5	2	6	CARB	T	2	ST	ICM_GMS	GMS-0006	GMS-0005
ST	Storegga Seep enrichment	65.5178	5.4747	721	5.0	-1	4	6	SARC	P	3	P	ICM_GMS	GMS-0014	GMS-0013
BS2	Black Sea nodule pink	44.7750	31.9922	225	0.1	8	4	5	MEDI	W	2	TEM	BPC_MET	MET004	MET003
GB4a	Guaymas 4484 1cm	27.0065	-111.4096	2000	1.0	2	4	6	CAMR	C	3	ST	ICM_GMS	GMS-0017	GMS-0018
GB4b	Guaymas 4484 4cm	27.0065	-111.4096	2000	5.0	50	4	3	CAMR	C	3	ST	ICM_GMS	GMS-0019	GMS-0020
ANT	Extinct Antarctic Seep	-65.4350	-61.4415	850	17.0	2	1	6	APLR	P	3	P	BPC_MET	MET002	MET001
BS1	Black Sea nodule black	44.7750	31.9922	225	0.1	8	4	5	MEDI	W	2	TEM	ICM_GMS	GMS-0016	GMS-0015
NS	Gullfaks - North Sea	61.1733	-2.2417	145	1.5	8	5	6	NECS	C	5	P	BPC_MET	MET006	MET005
HMMV	Håkon Mosby Mud Volcano	72.0032	14.7205	1263	1.5	-1	4	1	SARC	P	3	P	BPC_MET	MET008	MET007
KO	REGAB Pockmark - Kongo	-5.8106	9.7131	3172	3.0	3	1	5	ETRA	T	2	T	BPC_MET	MET010	MET009
JAP	Japan Trench	39.1059	143.8927	5347	5.0	1	2	3	KURO	W	2	ST	BPC_MET	MET012	MET011
HRB	Hydrate Ridge - Beggiatoa mat	44.5684	-125.1468	777	4.0	4	5	4	CCAL	C	3	TEM	BPC_MET	MET014	MET013
HRC	Hydrate Ridge - Calyptogena	44.5698	-125.1475	787	4.0	4	5	5	CCAL	C	3	TEM	BPC_MET	MET016	MET015
QS	Quepos Slide - Costa Rica	8.8500	-84.2148	400	5.0	9	2	3	CAMR	C	3	T	BPC_MET	MET018	MET017
NZA	Hikurangi (NZ) - Ampharetid bed	-41.7821	175.4020	1056	5.0	4	3	5	NEWZ	C	3	TEM	BPC_MET	MET020	MET019
NZB	Hikurangi (NZ) - Beggiatoa mat	-41.8458	175.6347	1058	5.0	4	3	4	NEWZ	C	3	TEM	BPC_MET	MET022	MET021
GB3	Guaymas Basin - 4489	27.0074	-111.4089	2000	6.0	85	4	6	CAMR	C	3	ST	BPC_MET	MET024	MET023
GB2	Guaymas Basin - 4486	27.0077	-111.4088	2000	7.0	25	4	6	CAMR	C	3	ST	BPC_MET	MET026	MET025
GB1	Guaymas Basin - 4483	27.0065	-111.4087	2000	9.0	15	4	4	CAMR	C	3	ST	BPC_MET	MET028	MET027
WO	White Oak River Estuary	34.7415	-77.1241	2	24.0	11	3	2	NWCS	C	4	ST	ICM_GMS	GMS-0002	GMS-0001
AB1	Aarhus Bay - GC174_16	56.1179	10.3482	15	149.5	8	2	3	NECS	C	5	TEM	BPC_MET	MET030	MET029
AB2	Aarhus Bay - GC174_17	56.1179	10.3482	15	169.5	8	3	2	NECS	C	5	TEM	BPC_MET	MET032	MET031
GoM3	Gulf of Mexico (deep/MC118)	28.5126	-88.2940	890	212.0	6	4	1	CARB	T	2	ST	ICM_GMS	GMS-0008	GMS-0007

DS5	Coastal Sand - North Sea	51.8781	0.9335	1	2.5	13	4	4	NECS	C	5	TEM	ICM_CFU	CFU_12	CFU_11
MM1	Coastal Sand - North Sea	53.4922	6.1400	0	0.3	8	0	6	NECS	C	5	TEM	ICM_CMM	CMM_11	CMM_02
MM2	Coastal Sand - North Sea	53.4922	6.1400	0	0.3	18	0	6	NECS	C	5	TEM	ICM_CMM	CMM_14	CMM_05
MM3	Coastal Sand - North Sea	53.4922	6.1400	0	0.3	17	0	6	NECS	C	5	TEM	ICM_CMM	CMM_17	CMM_08
CR1	Coral Reef Surface - Oahu	21.4667	-157.8000	1	1.0	25	0	6	NPTG	T	1	ST	ICM_CRS	CRS_06	CRS_01
CR2	Coral Reef Deep - Oahu	21.4667	-157.8000	1	50.0	25	0	6	NPTG	T	1	ST	ICM_CRS	CRS_07	CRS_04
AGW1	French Guiana Shallow Coast	5.5448	-53.1790	1	1.5	28	0	6	GUIA	C	5	T	ICM_AGW	n.a.	AGW_0001
AGW2	French Guiana Shallow Coast	5.5448	-53.1790	1	8.5	28	0	6	GUIA	C	5	T	ICM_AGW	n.a.	AGW_0002
AGW3	French Guiana Deep Coast	5.5428	-52.1974	52	1.5	28	0	6	GUIA	C	5	T	ICM_AGW	n.a.	AGW_0003
AGW4	French Guiana Deep Coast	5.5428	-52.1974	52	8.5	28	0	6	GUIA	C	5	T	ICM_AGW	n.a.	AGW_0004
LCR1	Caribbean Shallow Reef	17.9389	-67.0478	2	5.0	28	0	6	CARB	T	2	T	ICM_LCR	n.a.	LCR_0001
LCR2	Caribbean Deep Reef	17.8761	-67.0400	50	5.0	25	0	6	CARB	T	2	T	ICM_LCR	n.a.	LCR_0003
LCR3	South Argentina Intertidal	-42.4256	-64.1175	0	0.0	10	0	6	FKLD	C	4	TEM	ICM_LCR	n.a.	LCR_0015
VAG1	Chilean Coastal Sediment	-36.6900	-73.0700	15	2.5	13	0	6	CHIL	C	2	TEM	ICM_VAG	n.a.	VAG_0009
VAG2	Chilean Coastal Sediment	-36.6400	-73.0400	27	2.5	11	0	6	CHIL	C	2	TEM	ICM_VAG	n.a.	VAG_0010
VAG3	Chilean Coastal Sediment	-36.6000	-73.0000	35	2.5	12	0	6	CHIL	C	2	TEM	ICM_VAG	n.a.	VAG_0011
VAG4	Chilean Coastal Sediment	-36.5100	-73.1200	88	2.5	10	0	6	CHIL	C	2	TEM	ICM_VAG	n.a.	VAG_0012
ODP1	ODP Core - Peru Margin	-10.9833	-77.9500	150	250.0	14	1	5	CHIL	C	2	T	KCK_ODP	ODP_09	ODP_10
ODP2	ODP Core - Peru Margin	-10.9833	-77.9500	150	3015.0	15	3	1	CHIL	C	2	T	KCK_ODP	ODP_11	ODP_12
ODP3	ODP Core - Peru Margin	-10.9833	-77.9500	150	5035.0	15	4	1	CHIL	C	2	T	KCK_ODP	ODP_13	ODP_14
ODP4	ODP Core - Peru Margin	-10.9833	-77.9500	150	9145.0	17	3	1	CHIL	C	2	T	KCK_ODP	ODP_15	ODP_16
DS4	ODP Core - Peru Margin	-11.0645	-78.0778	262	3505.0	15	2	3	CHIL	C	2	T	ICM_CFU	CFU_08	CFU_07
LV1	Lau Hydrothermal Vent	-20.3167	-176.1363	2707	0.0	3	1	6	SPSG	T	1	T	ICM_ALR	ALR_09	ALR_01
LV2	Lau Hydrothermal Vent	-20.3179	-176.1374	2714	0.0	3	1	6	SPSG	T	1	T	ICM_ALR	ALR_10	ALR_02
LV3	Lau Hydrothermal Vent	-22.1807	-176.6012	1908	0.0	3	1	6	SPSG	T	1	T	ICM_ALR	ALR_12	ALR_04
LV4	Lau Hydrothermal Vent	-20.0530	-176.1337	2619	0.0	3	1	6	SPSG	T	1	T	ICM_ALR	ALR_16	ALR_08
LV5	Lau Hydrothermal Vent	-20.3167	-176.1363	2707	0.0	3	1	6	SPSG	T	1	T	ICM_ALR	ALR_18	ALR_17
LV6	Lau Hydrothermal Vent	-20.3167	-176.1363	2707	0.0	3	1	6	SPSG	T	1	T	ICM_ALR	ALR_20	ALR_19
LC1	Lost City Hydrothermal Vent	30.1240	-42.1193	827	0.0	7	1	6	NASW	W	1	ST	ICM_LCY	LCY_12	LCY_01
LC2	Lost City Hydrothermal Vent	30.1240	-42.1193	782	0.0	73	1	6	NASW	W	1	ST	ICM_LCY	LCY_14	LCY_03
LC3	Lost City Hydrothermal Vent	30.1240	-42.1193	735	0.0	81	1	6	NASW	W	1	ST	ICM_LCY	LCY_16	LCY_05
LC4	Lost City Hydrothermal Vent	30.1240	-42.1193	782	0.0	73	1	6	NASW	W	1	ST	ICM_LCY	LCY_18	LCY_07
ASV1	Azores Shallow Vent	37.7240	-25.3194	7	0.0	60	1	6	NASE	W	1	ST	ICM_ASV	n.a.	ASV_0007
ASV2	Azores Shallow Vent	37.7240	-25.3194	6	0.0	60	1	6	NASE	W	1	ST	ICM_ASV	n.a.	ASV_0008
ASV3	Azores Shallow Vent	38.2333	-26.6333	20	0.0	40	1	6	NASE	W	1	ST	ICM_ASV	n.a.	ASV_0015
ASV4	Azores Shallow Vent	38.2333	-26.6333	20	0.0	40	1	6	NASE	W	1	ST	ICM_ASV	n.a.	ASV_0016

*Methane concentrations are presented in categories: 0: 0-0.001 mM; 1: 0.001-0.01 mM; 2: 0.01-0.1 mM; 3: 0.1-1 mM; 4: 1-10 mM; 5: 10-100 mM **Sulfate concentrations are presented in categories: 1: 0-1 mM; 2: 1-2 mM; 3: 2-5 mM; 4: 5-10 mM; 5: 10-20 mM; 6: 20-30 mM

The ICoMM contextual geospatial and physicochemical parameters are available on the web (VAMPS website: <http://vamps.mbl.edu>. // MICROBIS website: <http://icomm.mbl.edu/microbis>). Additional data are from references (4, 5, 24, 25, 51-61)

Table S8: Qualitative comparison of culture-independent methods

Methane Seep	Organism	16S rRNA V6 region *	16S rRNA Full length **	CARD-FISH ***
Håkon Mosby mud volcano	ANME-1	-	-	-
Beggiatoa mat	ANME-2	+	-	-
	ANME-3	+++	+++	+++
Hydrate Ridge	ANME-1	++	++	++
Beggiatoa mat	ANME-2	+++	+++	+++
	ANME-3	+	+	n.d.
Hikurangi - New Zealand	ANME-1	-	-	-
Beggiatoa mat	ANME-2	+++	+++	+++
	ANME-3	++	++	+
Gullfaks - North Sea	ANME-1	+	-	-
Beggiatoa mat	ANME-2	+++	+++	+++
	ANME-3	+	-	-

* Sequenced using 454 pyrosequencing
in situ hybridization - not detected

** Sequenced using Sanger method
+ present ++ abundant

*** Catalyzed reporter deposition fluorescence
+++ dominant n.d. not determined

Table S9: Sequence read numbers of the ten most frequent OTU_{0.03} of key functional clades

DS1	DS2	DS3	GoM1	GoM2	ST	BS2	GB4a	GB4b	ANT	BS1	NS	HMMV	KO	JAP	HRB	HRC	QS	NZ1	NZ2	GB3	GB2	GB1	Total Reads	Clade	
9	0	92	1930	2506	11246	26	0	0	122	20428	17370	75	545	415	8938	4203	4343	4371	11647	0	245	0	88511	ANME2ab (OTU ₁₃₅₂)	
46	0	8	577	447	4	0	0	0	883	0	7	13956	5455	29	6736	1885	13	6174	3395	0	27	0	39642	ANME3	
13189	44	883	2577	14	0	30	45	81	9	17	0	0	0	2	438	1511	0	0	0	0	0	0	0	18840	ANME1
32	0	0	865	69	88	0	1	0	0	319	37	1	880	7022	3067	1359	114	133	18	0	56	0	14061	ANME2c	
0	0	538	890	111	0	10548	8	5	0	17	0	0	0	0	66	649	0	0	0	0	0	0	0	12832	ANME1b
1	0	28	361	335	1570	4	0	0	27	2580	1941	25	32	32	1040	536	627	637	1590	0	45	0	11411	ANME2ab	
106	0	492	3012	236	4	27	0	0	246	1	0	0	16	0	503	3811	0	1	0	0	0	0	0	8455	ANME1b
5	0	3	0	0	0	1	1552	3336	0	0	0	0	0	0	40	21	0	0	0	1	0	2	0	4961	ANME1
0	0	135	181	14	0	2329	1	0	0	0	0	0	0	0	13	194	0	0	0	0	0	0	0	2867	ANME1b
2383	3	33	193	0	0	4	5	53	2	0	0	0	0	0	40	140	0	0	0	0	0	0	0	2856	ANME1a
0	0	0	0	9	67	0	16	14	0	0	303	5488	114	73	130	61	2	2356	954	3	8	3	9601	Methylococcales (OTU ₂₂₀₆₄)	
0	0	0	0	0	0	0	0	0	0	0	3933	0	0	0	0	0	0	1	0	0	0	0	0	3934	Methylococcales
0	0	0	1	26	98	0	6	15	0	0	826	11	51	149	122	54	5	110	329	1	2	0	1806	Methylococcales	
0	0	2	1	12	37	0	12	0	0	0	40	802	11	7	26	11	0	215	128	1	7	0	1312	Methylococcales	
0	0	0	0	0	50	0	12	0	0	0	0	816	35	34	16	8	0	157	91	1	0	44	1264	Methylococcales	
0	0	0	0	0	0	0	0	0	0	0	454	0	0	0	0	0	0	0	0	0	0	0	454	Methylococcales	
0	0	0	0	1	3	0	3	0	0	0	1	47	5	2	11	2	1	276	35	0	1	0	388	Methylococcales	
0	0	0	0	15	77	0	11	10	0	0	61	3	2	24	21	10	0	10	50	2	1	0	297	Methylococcales	
0	0	0	3	2	77	0	6	0	0	0	1	8	0	16	11	3	16	4	11	0	0	0	158	Methylococcales	
0	0	0	0	0	0	0	0	0	0	0	1	92	0	0	0	0	0	0	0	0	0	0	93	Methylococcales	
0	0	0	1126	127	423	21	0	0	0	405	223	2	24	615	497	208	99	54	835	1	1	0	4661	Desulfobacterales (OTU ₄₄₅₄₀)	
9	0	7	147	85	145	22	2	0	6	3133	192	0	3	79	191	124	117	12	94	76	85	121	4650	Desulfobacterales	
0	0	0	0	0	162	1	0	0	0	2738	1	567	0	3	44	4	4	0	62	0	0	0	3586	Desulfobacterales	
0	0	0	2	24	238	0	61	0	0	0	754	2	66	496	691	145	9	7	169	54	86	0	2804	Desulfobacterales	
0	0	35	150	16	328	218	802	335	0	3	0	0	0	0	106	704	3	0	0	5	3	20	2728	Desulfobacterales	
0	0	1	0	12	8	0	0	0	15	0	43	310	341	306	96	16	27	242	931	4	6	65	2423	Desulfobacterales	
0	0	0	0	0	0	0	0	0	0	2163	0	73	0	0	0	0	0	0	0	0	0	0	2236	Desulfobacterales	
0	0	0	0	1	0	0	1	0	0	0	28	980	14	10	468	45	21	268	50	0	3	26	1915	Desulfobacterales	
0	0	0	0	0	5	0	0	0	0	0	0	1459	71	0	0	0	0	1	1	0	0	0	1537	Desulfobacterales	
1	0	0	707	79	309	11	0	0	0	35	23	0	0	58	93	40	2	7	121	0	0	0	1486	Desulfobacterales	
0	0	2	5	71	598	0	4	0	0	0	221	47	129	500	474	275	39	78	139	85	106	0	2773	Thiotrichales (OTU ₂₁₁₁₇)	
0	0	0	0	0	0	0	298	223	0	0	0	0	0	0	0	0	0	0	1	1	13	536	Thiotrichales		
0	0	0	1	17	34	0	0	0	0	1	5	12	10	127	4	7	0	27	51	3	1	0	300	Thiotrichales	
0	0	0	0	17	123	0	1	0	0	0	12	3	3	11	40	18	2	0	15	6	6	0	257	Thiotrichales	
0	0	0	0	0	1	0	9	0	0	0	1	22	18	0	4	0	0	80	14	0	0	0	149	Thiotrichales	
0	0	0	0	2	32	0	0	2	0	0	2	2	0	16	26	4	1	1	15	4	7	0	114	Thiotrichales	
0	0	0	0	0	0	0	2	0	0	0	0	0	5	0	1	0	0	82	15	0	2	0	107	Thiotrichales	
0	0	0	0	0	0	0	0	0	0	0	1	2	31	2	1	0	0	58	6	0	1	0	102	Thiotrichales	
0	0	0	0	21	0	0	0	0	0	0	0	0	1	31	4	1	0	0	11	28	0	0	97	Thiotrichales	
0	0	0	0	5	0	3	0	0	0	0	0	1	6	2	3	27	1	7	3	7	20	85	Thiotrichales		

The numbers correspond to observed sequence reads per sample of the ten most frequent OTU_{0.03} of the respective order.

The light green boxes depict relative single sequence OTU_{0.03} (SSO_{rel}). SSO_{rel} occur at least at one seep only once, but are more frequent at other seeps (1)

References

1. Gobet A, et al. (2012) Diversity and dynamics of rare and of resident bacterial populations in coastal sands. *ISME J* 6(3):542-553.
2. Gaidos E, Rusch A, & Ilardo M (2010) Ribosomal tag pyrosequencing of DNA and RNA from benthic coral reef microbiota: community spatial structure, rare members and nitrogen-cycling guilds. *Environ Microbiol* 13(5):1138-1152.
3. Hamilton TL, Peters JW, Skidmore ML, & Boyd ES (2013) Molecular evidence for an active endogenous microbiome beneath glacial ice. *ISME J* 7(7):1402-1412.
4. Biddle JF, et al. (2012) Anaerobic oxidation of methane at different temperature regimes in Guaymas Basin hydrothermal sediments. *ISME J* 6(5):1018-1031.
5. Treude T, et al. (2007) Consumption of Methane and CO₂ by Methanotrophic Microbial Mats from Gas Seeps of the Anoxic Black Sea. *Appl Environ Microbiol* 73(7):2271-2283.
6. Benjamini Y & Hochberg Y (1995) Controlling the False Discovery Rate: A Practical and Powerful Approach to Multiple Testing. *J Roy Stat Soc B Met* 57(1):289-300.
7. Harrison BK, Zhang H, Berelson W, & Orphan VJ (2009) Variations in Archaeal and Bacterial Diversity Associated with the Sulfate-Methane Transition Zone in Continental Margin Sediments (Santa Barbara Basin, California). *Appl Environ Microbiol* 75(6):1487-1499.
8. Dufrène M & Legendre P (1997) Species Assemblages And Indicator Species: The Need For A Flexible Asymmetrical Approach. *Ecol Monogr* 67(3):345-366.
9. Campbell BJ, Summers Engel A, Porter ML, & Takai K (2006) The versatile ε-proteobacteria: key players in sulphidic habitats. *Nat Rev Microbiol* 4(6):458-468.
10. Durbin AM & Teske A (2011) Microbial diversity and stratification of South Pacific abyssal marine sediments. *Environ Microbiol* 13(12):3219-3234.
11. Lloyd KG, et al. (2013) Predominant archaea in marine sediments degrade detrital proteins. *Nature* 496(7444):215-218.
12. Meng J, et al. (2014) Genetic and functional properties of uncultivated MCG archaea assessed by metagenome and gene expression analyses. *ISME J* 8(3):650-659.
13. Nunoura T, et al. (2013) Isolation and Characterization of a Thermophilic, Obligately Anaerobic and Heterotrophic Marine *Chloroflexi* Bacterium from a *Chloroflexi*-dominated Microbial Community Associated with a Japanese Shallow Hydrothermal System, and Proposal for *Thermomarinilinea lacunofontalis* gen. nov., sp. nov. *Microbes Environ* 28(2):228-235.
14. Paul K, Nonoh JO, Mikulski L, & Brune A (2012) "Methanoplasmatales," Thermoplasmatales-Related Archaea in Termite Guts and Other Environments, Are the Seventh Order of Methanogens. *Appl Environ Microbiol* 78(23):8245-8253.
15. Hubert C, et al. (2009) A Constant Flux of Diverse Thermophilic Bacteria into the Cold Arctic Seabed. *Science* 325(5947):1541-1544.

16. Dubinina G, Grabovich M, Leshcheva N, Rainey FA, & Gavril E (2011) Spirochaeta perfilievii sp. nov., an oxygen-tolerant, sulfide-oxidizing, sulfur- and thiosulfate-reducing spirochaete isolated from a saline spring. *Int J Syst Evol Microbiol* 61(1):110-117.
17. Parkes RJ, et al. (2014) A review of prokaryotic populations and processes in sub-seafloor sediments, including biosphere:geosphere interactions. *Mar Geol* 352(0):409-425.
18. Gies EA, Konwar KM, Beatty JT, & Hallam SJ (2014) Illuminating Microbial Dark Matter in Meromictic Sakinaw Lake. *Appl Environ Microbiol* 80(21):6807-6818.
19. Chevalier N, Bouloubassi I, Birgel D, Taphanel MH, & López-García P (2013) Microbial methane turnover at Marmara Sea cold seeps: a combined 16S rRNA and lipid biomarker investigation. *Geobiology* 11(1):55-71.
20. Jørgensen SL, et al. (2012) Correlating microbial community profiles with geochemical data in highly stratified sediments from the Arctic Mid-Ocean Ridge. *Proc Natl Acad Sci USA* 109(42):2846-2855.
21. Liu L, Yang J, Yu X, Chen G, & Yu Z (2013) Patterns in the Composition of Microbial Communities from a Subtropical River: Effects of Environmental, Spatial and Temporal Factors. *PLoS ONE* 8(11):e81232.
22. Ramette A & Tiedje JM (2007) Multiscale responses of microbial life to spatial distance and environmental heterogeneity in a patchy ecosystem. *Proc Natl Acad Sci USA* 104(8):2761-2766.
23. Konopka A (2009) What is microbial community ecology? *ISME J* 3(11):1223-1230.
24. Falden J, et al. (2014) Anaerobic methanotrophic community of a 5346-m-deep vesicomyid clam colony in the Japan Trench. *Geobiology* 12(3):183-199.
25. Ruff SE, et al. (2013) Microbial Communities of Deep-Sea Methane Seeps at Hikurangi Continental Margin (New Zealand). *PLoS ONE* 8(9):e72627.
26. Falden J, et al. (2013) Limitations of microbial hydrocarbon degradation at the Amon mud volcano (Nile deep-sea fan). *Biogeosciences* 10(5):3269-3283.
27. Huber JA, et al. (2007) Microbial Population Structures in the Deep Marine Biosphere. *Science* 318(5847):97-100.
28. Sogin ML, et al. (2006) Microbial diversity in the deep sea and the underexplored "rare biosphere". *Proc Natl Acad Sci USA* 103(32):12115-12120.
29. Schloss PD, Gevers D, & Westcott SL (2011) Reducing the Effects of PCR Amplification and Sequencing Artifacts on 16S rRNA-Based Studies. *PLoS ONE* 6(12):e27310.
30. Quince C, et al. (2009) Accurate determination of microbial diversity from 454 pyrosequencing data. *Nat Meth* 6(9):639-641.
31. Huse SM, Welch DM, Morrison HG, & Sogin ML (2010) Ironing out the wrinkles in the rare biosphere through improved OTU clustering. *Environ Microbiol* 12(7):1889-1898.

32. Edgar RC, Haas BJ, Clemente JC, Quince C, & Knight R (2011) UCHIME improves sensitivity and speed of chimera detection. *Bioinformatics* 27(16):2194-2200.
33. Hill TCJ, Walsh KA, Harris JA, & Moffett BF (2003) Using ecological diversity measures with bacterial communities. *FEMS Microbiol Ecol* 43(1):1-11.
34. Chao A (1984) Nonparametric Estimation of the Number of Classes in a Population. *Scand J Stat* 11(4):265-270.
35. Bray JR & Curtis JT (1957) An Ordination of the Upland Forest Communities of Southern Wisconsin. *Ecol Monogr* 27(4):326-349.
36. Kruskal JB (1964) Nonmetric multidimensional scaling: A numerical method. *Psychometrika* 29(2):115-129.
37. Gower JC (1975) Generalized Procrustes analysis. *Psychometrika* 40:33-51.
38. Legendre P & Legendre L (1998) *Numerical Ecology* (Elsevier Science B.V., Amsterdam) 2nd Ed p 853.
39. Nekola JC & White PS (1999) The distance decay of similarity in biogeography and ecology. *J Biogeogr* 26(4):867-878.
40. Rosenzweig M, L. (1995) *Species Diversity in Space and Time* (Cambridge University Press).
41. Zinger L, Boetius A, & Ramette A (2014) Bacterial taxa-area and distance-decay relationships in marine environments. *Mol Ecol* 23(4):954-964.
42. Fruchterman TMJ & Reingold EM (1991) Graph drawing by force-directed placement. *Software Pract Exper* 21(11):1129-1164.
43. Oksanen J, et al. (2012) vegan: Community Ecology Package.
44. Roberts DW (2012) labdsv: Ordination and Multivariate Analysis for Ecology).
45. Magnusson A (2011) Interface between GMT Map-Making Software and R.
46. Butts CT, Handcock MS, & Hunter DR (2007) Network: classes for relational data.
47. Schreiber L, Holler T, Knittel K, Meyerdierks A, & Amann R (2010) Identification of the dominant sulfate-reducing bacterial partner of anaerobic methanotrophs of the ANME-2 clade. *Environ Microbiol* 12(8):2327-2340.
48. Kleindienst S, Ramette A, Amann R, & Knittel K (2012) Distribution and in situ abundance of sulfate-reducing bacteria in diverse marine hydrocarbon seep sediments. *Environ Microbiol* 14(10):2689-2710.
49. Holler T, et al. (2011) Thermophilic anaerobic oxidation of methane by marine microbial consortia. *ISME J* 5(12):1946-1956.
50. Quast C, et al. (2013) The SILVA ribosomal RNA gene database project: improved data processing and web-based tools. *Nucleic Acids Res* 41(D1):D590-D596.

51. Pop Ristova P, et al. (2012) Bacterial diversity and biogeochemistry of different chemosynthetic habitats of the REGAB cold seep (West African margin, 3160 m water depth). *Biogeosciences* 9(12):5031-5048.
52. Lloyd KG, Alperin MJ, & Teske A (2011) Environmental evidence for net methane production and oxidation in putative ANaerobic MEthanotrophic (ANME) archaea. *Environ Microbiol* 13(9):2548-2564.
53. Sommer S, Linke P, Pfannkuche O, Niemann H, & Treude T (2010) Benthic respiration in a seep habitat dominated by dense beds of ampharetid polychaetes at the Hikurangi Margin (New Zealand). *Mar Geol* 272(1-4):223-232.
54. Lloyd KG, et al. (2010) Spatial Structure and Activity of Sedimentary Microbial Communities Underlying a *Beggiatoa* spp. Mat in a Gulf of Mexico Hydrocarbon Seep. *PLoS ONE* 5(1):e8738.
55. Lichtschlag A, Felden J, Brüchert V, Boetius A, & de Beer D (2010) Geochemical processes and chemosynthetic primary production in different thiotrophic mats of the Haakon Mosby Mud Volcano (Barents Sea). *Limnol Oceanogr* 55(2):931-949.
56. Grünke S, et al. (2010) Novel observations of Thiobacterium, a sulfur-storing Gammaproteobacterium producing gelatinous mats. *ISME J* 4(8):1031-1043.
57. Aquilina A, et al. (2010) Biomarker indicators for anaerobic oxidizers of methane in brackish-marine sediments with diffusive methane fluxes. *Org Geochem* 41(4):414-426.
58. Niemann H, et al. (2009) Biogeochemistry of a low-activity cold seep in the Larsen B area, western Weddell Sea, Antarctica. *Biogeosciences* 6(11):2383-2395.
59. Wegener G, et al. (2008) Biogeochemical processes and microbial diversity of the Gullfaks and Tommeliten methane seeps (Northern North Sea). *Biogeosciences* 5(4):1127-1144.
60. Knittel K, Lösekann T, Boetius A, Kort R, & Amann R (2005) Diversity and Distribution of Methanotrophic Archaea at Cold Seeps. *Appl Environ Microbiol* 71(1):467-479.
61. Longhurst A, Sathyendranath S, Platt T, & Caverhill C (1995) An estimate of global primary production in the ocean from satellite radiometer data. *J Plank Res* 17(6):1245-1271.